Diffraction of light from thin-film polymethylmethacrylate opaline photonic crystals

S. G. Romanov, T. Maka, and C. M. Sotomayor Torres
Institute of Materials Science and Department of Electrical and Information Engineering, University of Wuppertal, Gaußstraße 20, 42097 Wuppertal, Germany

M. Müller* and R. Zentel*
Institute of Materials Science and Department of Chemistry, University of Wuppertal, Gaußstraße 20, 42097 Wuppertal, Germany

D. Cassagne, J. Manzanares-Martinez, and C. Jouanin†
Groupe d'Etude des Semiconducteurs, CC074, Université Montpellier II, Place Bataillon, 34095, Montpellier Cedex 05, France
(Received 3 October 2000; published 11 April 2001)

Photonic crystals in the form of large area thin films consisting of closely packed polymethylmethacrylate beads were sedimented on glass substrates. The high ordering of the opaline films made it possible to observe a number of fine features in the optical diffraction, including Fabry-Perot oscillations of the reflectivity and branching of the angular dispersion of the Bragg resonances with increase of the angle of incidence of the light beam. Results of calculations of the photonic band structure and simulations of the reflectance spectra agree well with experimental observations.

DOI: 10.1103/PhysRevE.63.056603 PACS number(s): 42.70.Qs

I. INTRODUCTION

Photonic crystals are periodic dielectric structures designed to control the propagation of electromagnetic (EM) waves by defining allowed and forbidden energy bands in the photon dispersion spectrum (see, e.g., [1]). To make use of the absence of propagating EM modes, e.g., to suppress the spontaneous emission in certain frequency ranges, highly crystalline three-dimensional photonic band gap (PBG) materials are essential. One natural route toward three-dimensional photonic crystals with a complete PBG is to start with the opaline structure—a perfect self-assembled package of identical colloidal nanoparticles—, use it as a template for infilling with a high-refractive-index (RI) material [2], and then extract the high-RI replica of this nanocomposite (inverted opaline structure) [3]. The success of this approach depends on having high-quality opaline templates [4] as well as effective and low-cost technologies suitable for mass production.

The experimental assessment of incomplete photonic crystals includes an examination of the evolution of the Bragg diffraction resonance with changing angle of light incidence. The band structure of bare opal (see, e.g., [5]) shows a number of band crossings occurring in the lowest band gap when the wave vector circulates over the Brillouin zone. Correspondingly, an important criterion for the quality of a three-dimensional photonic crystal might be the possibility of resolving the splitting of the diffraction resonance at crossing points. In opals studied so far the unambiguous assignment of resonances coming from different crystallographic planes was made possible only by cutting the opals along the corresponding planes [6] because the clear resolution of the Bragg peak at high angles of light incidence was obscured due to insufficient ordering of opals. But even at the normal incidence of light the Bragg resonance was distorted by a contribution from defects, the number of which has been suggested to be typically as high as one defect per hundred unit cells [6].

As a rule of thumb, the quality of opal can be improved by increasing the aspect ratio, i.e., the ratio of the area to the thickness, as proved by experiments on thin packages of polymer beads [7,8]. On the other hand, there should be a sufficient number of layers in the opaline structure to form a band gap structure in the direction perpendicular to the film plane. The homogeneity of the film as a whole is characterized by Fabry-Perot oscillations, whose period depends on the film thickness and the index of refraction. To observe such oscillations with bulk opals single domain spectroscopy has been used [9], which implies the use of an optical microscope with a noncollimated beam to separate the signal from a single crystallite that is accidentally suitable for measurements.

In this paper we report studies of the Bragg resonance splitting and Fabry-Perot oscillations observed in the reflectance from thin opaline films using a beam with up to 1 cm^2 cross section. The observation of photonic band branching is particularly difficult in direct opals formed by dielectric spheres in air due to the weak refractive index contrast, and it requires high-quality samples. We demonstrate that this effect is strongly localized in the reciprocal space around the U point using a careful study of the band structures along the Γ-L and Γ-X lines. In Sec. I we briefly describe the polymethylmethacrylate (PMMA) opaline films and the measurement procedure. In Sec. II the angular resolved reflectance spectra of opaline films are analyzed in terms of correspondence to the Bragg law and to the numerically calculated band structure. The third part discusses specific features of Fabry-Perot oscillations in opaline films.

*Present address: Institute of Organic Chemistry, University of Mainz, Duesbergweg 10-14, 55099 Mainz, Germany.

†Deceased.

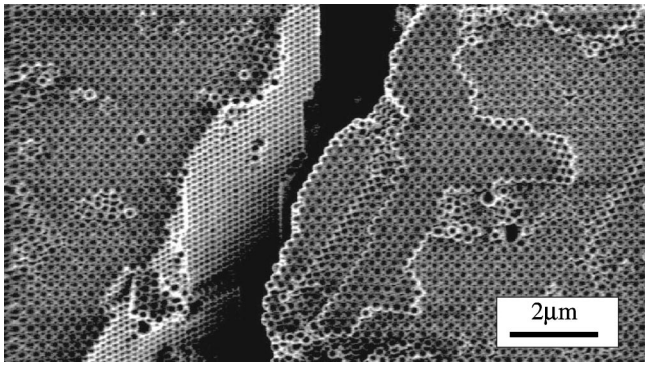

FIG. 1. SEM micrograph showing a film of fcc packed PMMA balls on a glass substrate. Note the alignment of packages in different blocks.

II. EXPERIMENTAL TECHNIQUES

PMMA beads with a mean diameter of 290 nm were prepared by modified emulsion polymerization from the monomer solution [10]. The bead diameter was controlled by varying the polymerization time. Bead suspensions were spread over hydrophilized glass microscope slides or silicon wafers over areas of several square centimeters, where the sediment self-assembles in a face-centered cubic (fcc) package with the (111) growth direction perpendicular to the substrate. The details of the chemical routine are given elsewhere [11]. A high level of package crystallinity was achieved for films with various diameters of beads and numbers of bead layers. Scanning electron microscope (SEM) inspection shows the deviation from the mean ball diameter to be less than 10% (Fig. 1) but smaller variation exists on a shorter length scale. These thin-film polymeric opaline crystals consist of ca. 10–40 monolayers and possess monocrystalline domains extending over hundreds of micrometers. However, the overall disorientation of domains over the film is small enough to produce a homogeneous coloration over an area of several square centimeters. The refractive index of PMMA is 1.489 and the filling factor of balls in the opaline film was assumed to be $f_{\mathrm{ball}}=0.74$.

Standard angular resolved reflectance/transmission measurements were carried out to study the PBG effect along the [111] direction in the opal photonic crystal [12,13]. An area of the sample from 0.1 to 1 cm^2 was illuminated with a well-collimated beam of white light and the scattered light was collected within a solid angle of 2° to take the anisotropy of the Bragg resonance into account. The angular dispersion of the stop band was studied by changing the angle of incidence θ between the beam and the (111) axis of the fcc crystal from 5° to 70° and by collecting the scattered light in the Bragg configuration.

III. BAND BRANCHING

Reflectance spectra of a representative PMMA opaline film collected at different angles θ are shown in Fig. 2. The relative stop band width of $\Delta E/E_0 \approx 5\%$ is determined as the full width at half maximum (FWHM) from the Bragg diffraction resonance reflectance at $\theta \approx 0°$. A similar FWHM of 6.7% was extracted from the transmission spectrum.

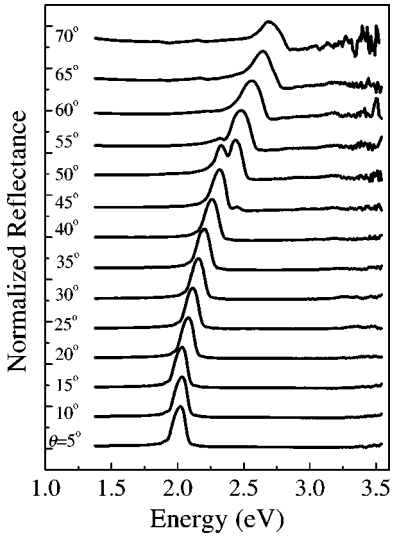

FIG. 2. Angle resolved reflectance spectra of PMMA opal film for angles between 5° and 70° from bottom to top with a 5° step.

The relative gap width along the (111) direction calculated by the plane wave method is about 6.3% [5]. This value is very close to the experimentally observed FWHM of the Bragg peak, probably due to the relatively low contribution from defects of the photonic crystal to the total transmission.

Splitting of the Bragg resonance into two peaks was observed for external angles between $\theta \approx 45°$ and 55°. This behavior can be attributed to the (200) Bragg reflection, when the specular conditions for reflectance are satisfied for both (111) and (200) sets of planes. The Bragg condition for (*hkl*) planes is given by

$$\lambda_{hkl}=2d_{hkl}n_{\mathrm{eff}}\sqrt{1-\sin^2 r_{hkl}},$$

where d_{hkl} is the distance between (*hkl*) planes, r_{hkl} is the internal angle between the wave vector and the $[hkl]$ direction, and n_{eff} is an effective refractive index. It can be estimated with the effective medium approximation that $n_{\mathrm{eff}}=n_{\mathrm{ball}}f_{\mathrm{ball}}+n_{\mathrm{air}}(1-f_{\mathrm{ball}})$ [14], where f_{ball} is the filling fraction of the volume occupied by the beads, and n_{ball} and n_{air} are the refractive indices of beads and air, respectively. Here the refractive index of the PMMA beads is taken to be $n_{\mathrm{ball}}=1.489$ and the filling factor is $f_{\mathrm{ball}}=0.74$, so we have $n_{\mathrm{eff}}=1.362$. θ is the external angle between the incident wave and the normal to the (111) surface of the film; the internal angle r_{111} is given by the Snell law $n_{\mathrm{air}}\sin\theta=n_{\mathrm{eff}}\sin r_{111}$. Since the angle between the (111) and (200) planes is 54.74°, $r_{200}=54.74°-r_{111}$. Figure 3 shows the angular dependence of the Bragg resonances from the (111) and (200) planes. We considered the beads to have a mean diameter of 282 nm in good agreement with the SEM images. According to whether a reflection peak is closer to the (111) or (200) Bragg curve, it can be associated with one of the two families of lattice planes. Thus, double peaks appear in the vicinity of the crossing between the two Bragg dependences obtained at $\theta=51.84°$.

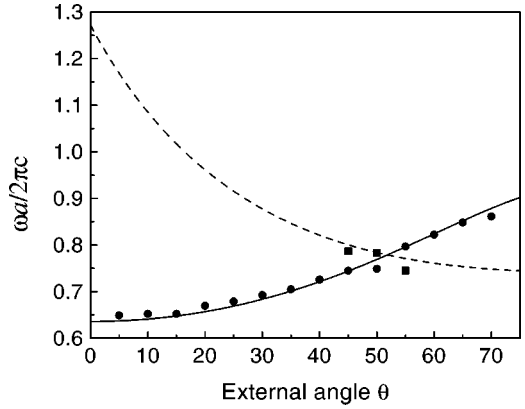

FIG. 3. Bragg law predictions for the diffraction from (111) and (200) planes against the external angle of incidence, denoted by solid and dashed lines, respectively. Circles and squares indicate experimental data associated with the (111) and (200) planes, respectively.

The explanation based on the Bragg law is not sufficient to fully interpret the experimental curves for two main reasons. First, double peaks appear only at certain incident angles. Second, near the crossing of the curves for the (111) and (200) planes the positions of the peak maxima do not follow the Bragg law exactly. To obtain a better understanding of this phenomenon, we consider an exact band structure calculation and associate band gaps and crystallographic planes using the Laue formulation of the diffraction condition [15]. The [111] and [200] directions are associated with the Γ-L and Γ-X directions of the reciprocal lattice, respectively. The existence of double peaks can be explained by considering the displacement of the internal wave vectors in the (ΓLX) plane in the reciprocal space of the fcc structure, as shown in Fig. 4. The Laue condition is satisfied if and only if the tip of the internal wave vector lies on a plane that is the perpendicular bisector of a line joining the Γ point to a reciprocal lattice point. Several k vectors can satisfy this condition at the same time according to the reciprocal lattice point considered. In Fig. 4 we show bisector planes that satisfy the Laue condition for diffraction at the (111) and (200) planes, respectively. These planes limit the first Brillouin zone (FBZ). For a given internal angle r_{111}, two wave vectors k and k' satisfying the Laue condition are indicated. They correspond to diffraction at (111) and (200) planes, respectively. Notice that the k' vector is outside the FBZ. Its position can be associated with a point inside the FBZ, but for clarity we just consider its continuous evolution in the reciprocal space along the (XU) straight line inside and outside the FBZ. Likewise, we consider the evolution of the tip of the k vector along the LU straight line. Figure 5 shows the band structure calculated along this line. Band structure calculations were carried out using the plane wave method in a similar way to Refs. [5], [16]. 1067 plane waves of the reciprocal lattice were used to obtain good convergence. Using the Snell law to define the internal angle, we plotted the positions of the experimental peaks we associate with (111) diffraction. They are in good agreement with the gap position. It is important to note that the gap exists for a large range of k vectors along this line. Figure 6 shows the band structure along the XU line; only the three peaks associated with the (200) planes are indicated. These peaks exist only in the vicinity of the U point and there is good agreement with the band structure calculation since the gap along this line is open only in the vicinity of the U point. This gives a clear explanation of the existence of double peaks only for exter-

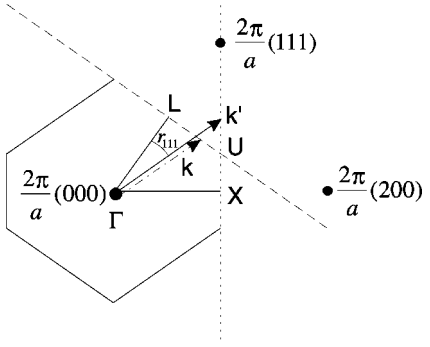

FIG. 4. (ΓLX) plane of the fcc reciprocal space. The bisector planes indicated by the dashed and the dotted lines correspond to the positions of the tips of wave vectors that satisfy the Laue condition for diffraction at the (111) and (200) planes, respectively. For a given internal angle r_{111}, two wave vectors k and k' that satisfy the Laue condition are indicated. It is worth noting that the k' vector is outside the first Brillouin zone.

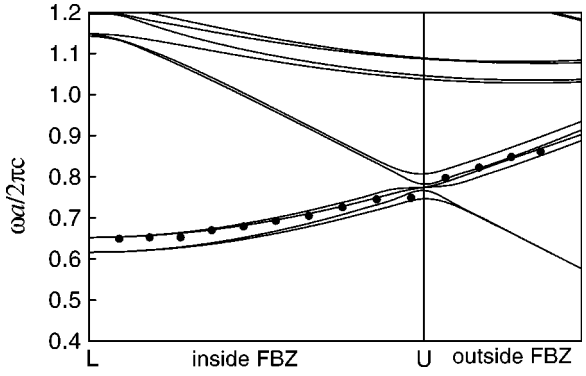

FIG. 5. Photonic band structure (solid lines) calculated along the LU line inside and outside the first Brillouin zone. The circles indicate the experimental peaks associated with (111) planes.

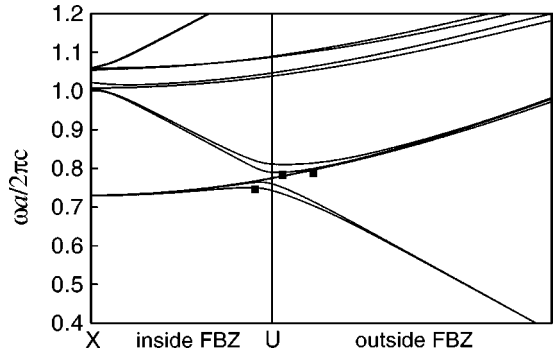

FIG. 6. Photonic band structure (solid lines) calculated along the XU line inside and outside the first Brillouin zone. The squares indicate the experimental peaks associated with (200) planes.

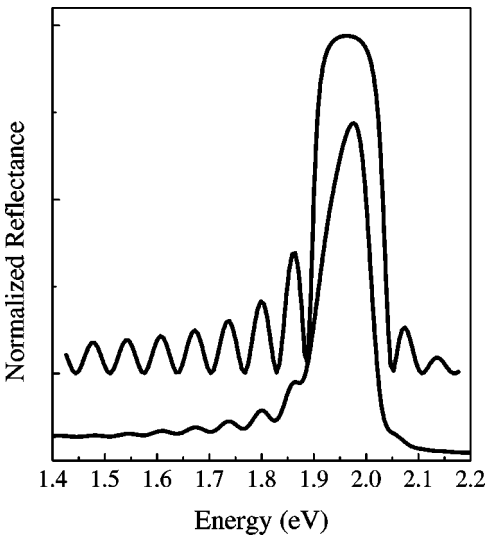

FIG. 7. Fabry-Perot oscillations of the reflectance near the Bragg resonance. Experimental curve for the sample $n_{bead}=1.49$ and $D=289$ nm (lower graph) and theoretical modeling with parameters $n_{ball}=1.42$, $D=292$ nm, and a thickness of 45 layers (upper graph).

nal angles near $\theta=51.84°$, which corresponds to internal angles near the *U* point. Moreover, the multiple band mixing that occurs at the *U* point decreases the frequency of the bands. This phenomenon is well known in solid state physics; it explains the deformation of the bands near the *U* point. The shift between the position of the experimental peaks and the Bragg curves of Fig. 3 near the crossing point occurs because the Bragg law does not take the band mixing into account. Therefore, by making reference to the band structure of these materials, we can explain the presence of double peaks by photonic band branching at the *U* point of the Brillouin zone.

An alternative explanation has been given for the double peak in the reflectance spectrum in the (100) direction as the result of stacking faults in the fcc lattice [6]. In our case the experimental conditions are quite different from those in Ref. [6], namely, the refractive index contrast is much higher (1.5:1 against 1.45:1.47) and the spectrum was measured under inclined light propagation with regard to the sample surface, both conditions that impose stronger scattering. Nevertheless, the evolution of this feature with increasing angle and the coincidence with the band structure calculations lead us to argue in favor of branching of the angular dispersion. In addition, below is another proof of the better quality of the lattice in opaline film over that in bulk opal.

IV. FABRY-PEROT OSCILLATIONS

The main Bragg peak in the reflectance spectrum of the PMMA opaline film is accompanied by a number of oscillations of the reflectance intensity predominantly on the low-energy side of the spectrum (Fig. 7). These oscillations can be understood as Fabry-Perot oscillations occurring due to the interference of the light reflected by opposite surfaces of the film. In our case, the Fabry-Perot oscillations are seen when studying the reflectance over a square centimeter area, which, apparently, is the consequence of the thickness homogeneity and similarity of orientation of the opaline structure. A decrease in the spot size from 1 cm^2 by a factor of 1000 results in an increase of the relative magnitude of oscillations by a factor of 3. If we increasing the RI of the substrate by using Si instead of SiO_2, the Fabry-Perot oscillations appear much more pronounced due to the stronger reflectance from the film-substrate interface.

Comparison between theoretical and experimental results is possible only if the exact number of layers in the sample is known. The reflectance spectra of films with different numbers of layers were calculated by using the three-dimensional (3D) transfer matrix method [17]. The calculated period of the Fabry-Perot oscillations was found to coincide with experimental values for a film thickness of 45 bead layers. This case is shown in Fig. 7, which compares the experimental and theoretical reflectance curves. There is very good agreement on the position of the Fabry-Perot oscillations. For frequencies below the gap, the amplitude of the oscillations increases toward the Bragg resonance for both curves. Above the gap, the calculated amplitudes are smaller, whereas they are not detected in the experiment. This gives good qualitative agreement for the amplitude evolution. It is worth noting that a 1D modeling of the reflection properties does not reproduce correctly the amplitude of the Fabry-Perot oscillations and cannot take this effect into account [9]. This variation of the amplitude of Fabry-Perot oscillations can be explained by a variation of the effective index of the material near the photonic band gap. The good agreement with theory, which considers a perfect arrangement of spheres, underlines the high quality of the thin-film sample.

The periodicity of Fabry-Perot oscillations depends on the product of the thickness of the opaline film and the effective RI of the structure. Changing the angle results in an increase of the optical path; however, there were no essential changes observed in the oscillation period. Apparently, the increase of the path length is balanced by the decrease of the effective RI, which occurs due the decrease of the package density when deviating from the (111) direction. Correspondingly, the dependence of frequency upon changing path length is canceled out.

V. CONCLUSION

In summary, polymer beads have been synthesized using a modified emulsion polymerization technique and thin-film opaline photonic crystals have been prepared from PMMA beads deposited on glass substrates The polymer opaline films have several advantages over silica opals: (i) they can be prepared with different dopants (e.g., fluorescent dyes), (ii) after infilling the organic template can be softly dissolved away from the nanocomposite [3,18,19], and (iii) polymer beads can be made nanostructured themselves during the synthesis [4]. Moreover, 3D photonic crystals prepared in the thin-film form can overcome the problem of integration with other components of optoelectronic devices. Certain modification of the sedimentation procedure can further improve the ordering of opaline films [4].

The level of quality of the ball package achieved made it possible to observe branching of the Bragg peak dispersion and oscillations of the reflectance due to the finite thickness of the structure. Comparisons between experimental results for real materials and theoretical calculations for perfect structures yield very good agreement and give a clear physical explanation of both the photonic band branching at high incident angles and the variation of the amplitude of Fabry-Perot oscillations.

We recently became aware of a study of multiple Bragg diffraction in high-contrast inverse opals formed by air spheres in titania (TiO_2) by van Driel and Vos [20]. In PMMA opals the contrast between the components air/PMMA is weak compared to that in inverse opals air/TiO_2, which makes the observation of photonic band branching difficult and shows the high quality of our samples.

ACKNOWLEDGMENT

This work was supported by the EU IST Project PHOBOS Grant No. 19009.

[1] *Microactivities and Photonic Bandgaps: Physics and Applications*, edited by J. Rarity and C. Weisbuch (Kluwer, Dordrecht, 1996); special issue of J. Lightwave Technol. **17** (1999).

[2] S. G. Romanov and C. M. Sotomayor Torres, in *Handbook of Nanostructured Materials and Technology*, edited by H. S. Nalwa, (Academic, New York, 1999), Vol. 4, Chap. 4, pp. 231–323.

[3] J. E. G. Wijnhoven and W. L. Vos, Science **281**, 802 (1998); A. A. Zakhidov, R. H. Baughman, Z. Iqbal, C. Cui, I. Khayrullin, S. O. Dantas, J. Marti, and V. G. Raichenko, *ibid.* **282**, 897 (1998).

[4] Y. Xia, B. Gates, Y. Yin, and Y. Lu, Adv. Mater. **12**, 693 (2000).

[5] A. Reynolds, F. López-Tejeira, D. Cassagne, F. J. García-Vidal, C. Jouanin, and J. Sánchez-Dehesa, Phys. Rev. B **60**, 11 422 (1999).

[6] Y. A. Vlasov, V. N. Astratov, A. V. Baryshev, A. A. Kaplianskii, O. Z. Karimov, and M. F. Limonov, Phys. Rev. E **61**, 5784 (2000).

[7] Y. Xia, B. Gates, and S. H. Park, J. Lightwave Technol. **17**, 1956 (1999).

[8] R. M. Amos, J. G. Rarity, P. R. Tapser, T. J. Shepherd, and S. C. Kitson, Phys. Rev. E **61**, 2929 (2000).

[9] Yu. A. Vlasov, M. Deutsch, and D. J. Norris, Appl. Phys. Lett. **76**, 1627 (2000).

[10] J. W. Goodwin, J. Hearn, and C. C. Ho, Colloid Polym. Sci. **252**, 464 (1974).

[11] M. Müller, R. Zentel, T. Maka, S. G. Romanov, and C. M. Sotomayor Torres, Chem. Mater. **12**, 2508 (2000).

[12] C. López, H. Míguez, L. Vázquez, F. Meseguer, R. Mayoral, and M. Ocaña, Superlattices Microstruct. **22**, 399 (1997).

[13] S. G. Romanov, A. V. Fokin, V. I. Alperovich, N. P. Johnson, and R. M. De La Rue, Phys. Status Solidi B **164**, 169 (1997).

[14] W. L. Vos, R. Sprik, A. von Blaaderen, A. Imhof, A. Lagendijk, and G. H. Wegdam, Phys. Rev. B **53**, 16 231 (1996); R. D. Pradhan, I. I. Tarhan, and G. H. Watson, *ibid.* **54**, 13 721 (1996).

[15] N. W. Ashcroft and N. D. Mermin, *Solid State Physics* (Saunders, New York, 1976).

[16] K. M. Ho, C. T. Chan, and C. M. Soukoulis, Phys. Rev. Lett. **65**, 3152 (1990).

[17] J. B. Pendry and A. MacKinnon, Phys. Rev. Lett. **69**, 2772 (1992); P. M. Bell, J. B. Pendry, L. Martin Moreno, and A. J. Ward, Comput. Phys. Commun. **85**, 306 (1995).

[18] S. H. Park, D. Qin, and Y. Xia, Adv. Mater. **10**, 1028 (1998).

[19] M. Müller, R. Zentel, T. Maka, S. G. Romanov, and C. M. Sotomayor Torres, Adv. Mater. **12**, 1499 (2000).

[20] H. M. van Driel and W. L. Vos, Phys. Rev. B **62**, 9872 (2000).